AGULHAS CURRENT

J. R. E. Lutjeharms, University of Cape Town, Rondebosch, South Africa

Copyright © 2001 Academic Press

doi:10.1006/rwos.2001.0365

Introduction

The greater Agulhas Current forms the western boundary system of the circulation in the South Indian Ocean. Contrary to the flow of comparable subtropical gyres in other ocean basins, the sources of the Agulhas Current are interrupted by a substantial barrier, the island of Madagascar. This leads to the formation of two minor western boundary flows, the East Madagascar Current and the Mozambique drift. Once fully constituted off the coast of south-eastern Africa, the Agulhas Current proper can be considered to consist of two distinct parts: the northern and the southern current. The northern part flows along a steep continental shelf and its trajectory is extremely stable. The southern part flows along the wide shelf expanse of the Agulhas Bank and by contrast meanders widely. South of the African continent the Agulhas Current retroflects in a tight loop, with most of its waters subsequently flowing eastward as the Agulhas Return Current. This loop configuration is unstable and at irregular intervals it is pinched off to form a detached Agulhas ring. These rings, carrying warm and salty Indian Ocean water, drift into the South Atlantic Ocean. Some cross the full width of this ocean in the next 2–3 years, whereas many are dissipated within 5 months of being spawned. The Agulhas Return Current flows back into the South Indian Ocean along the Subtropical Convergence. This juxtaposition generates considerable mesoscale turbulence in the form of meanders and an assortment of eddies. Water from the Agulhas Return Current leaks northward, back into the subtropical gyre, along its full length. By about 70°E all Agulhas water has been lost to the eastward flow that subsequently continues as the South Indian Ocean Current.

Importance

Historically the Agulhas Current was one of the first ocean currents to receive a great deal of scientific attention. It was described in some detail as early as 1766 by Major James Rennell, preeminent British geographer at the time. This was followed by wide-ranging investigations by Dutch mariners such as Van Gogh and Andrau in the 1850s. This early interest was motivated purely by nautical concerns, the Agulhas Current constituting a formidable impediment to vessels sailing to India and to the East. Fundamental studies by German investigators dominated research on the Agulhas Current region in the 1930s, but this endeavour was terminated by the Second World War. During the past few decades a renaissance in interest in this current has occurred for totally different reasons.

It has been demonstrated that the greater Agulhas Current system (**Figure 1**) has a marked influence on the climate variability over the southern African subcontinent. It has also been shown that this current is a key link in the exchanges of water between ocean basins and thus probably has a special role in the oceans' influence on global climate. This renewed interest has stimulated a number of research cruises, the placement of current meter moorings, investigations by satellite remote sensing, as well as theoretical and modeling studies, all leading to an enormous increase in knowledge of the Agulhas Current.

Large-scale Circulation

The Agulhas Current forms part of the overall circulation of surface waters in the South Indian Ocean that is anticyclonic, i.e., anticlockwise in the Southern Hemisphere (**Figure 2**). On its eastern side, the equatorward flow is weak and dispersed, whereas the recirculation in the South West Indian Ocean is particularly strongly developed, penetrating to 1000 m depth at its centre. The southern border to the circulation is the Subtropical Convergence. This strong thermohaline front at roughly 41°S separates the characteristic flows and water masses of the subtropical gyre and those of the Antarctic Circumpolar Current that lies to the south. Along the Subtropical Convergence, the Agulhas Return Current and the South Indian Ocean Current carry their respective water masses eastward. To the north the gyral circulation is closed by the South Equatorial Current that is found between about 10° and 25°S and carries water from east to west.

At the eastern shores of Madagascar, the South Equatorial Current splits into a northern and a southern limb of the East Madagascar Current; about 70% going north along this shoreline, 30%

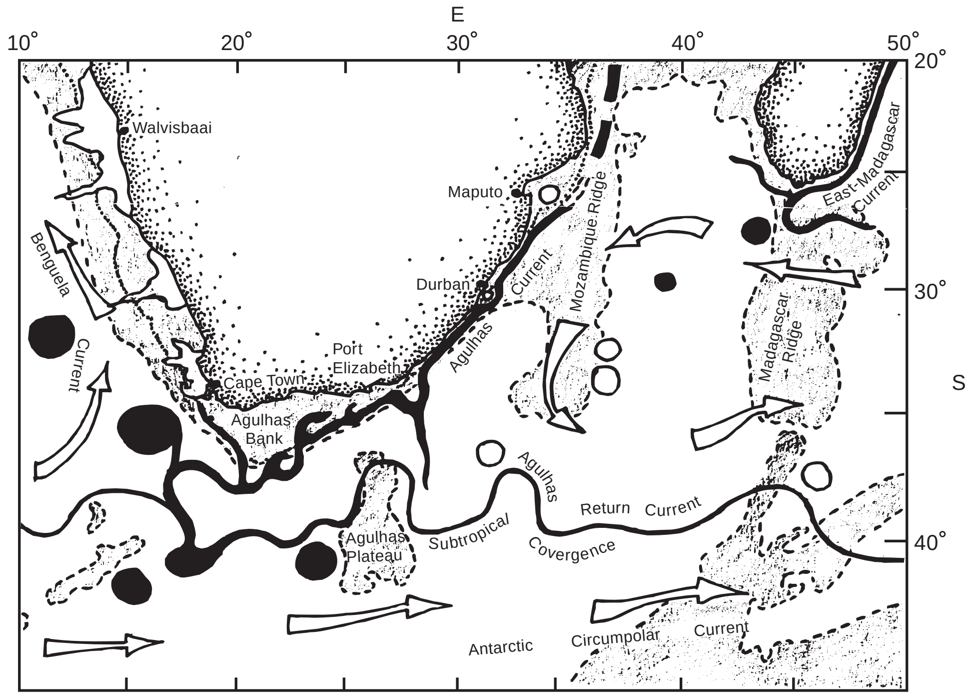

Figure 1 A conceptual portrayal of the greater Agulhas Current. Ocean regions shallower than 3000 m have been shaded. Intense currents are black, whereas the general background circulation is shown by open arrows. Cyclonic eddies are open; anticyclonic rings and eddies are black. Note the stability of the northern Agulhas Current, the meanders of the southern Agulhas Current, the tight retroflection loop, and the continuously weakening eastward flow of the Agulhas Return Current along the Subtropical Convergence. Agulhas rings (black) are advected by the Benguela Current past the extensive coastal upwelling off south-western Africa.

heading south. Most of that heading north eventually reaches the east coast of the African continent, where it forms the East African Coastal Current. There is some leakage from the Mozambique Channel and from the southern limb of the East Madagascar Current into the Agulhas Current, but most of the Agulhas Current's waters come from the subgyre of the South West Indian Ocean (see **Figure 2**). The Agulhas Current itself is narrow, deep, and fast; a typical western boundary current. All these surface currents are driven largely by the reigning wind systems.

The wind systems over the South West Indian Ocean fall largely outside the influence of the

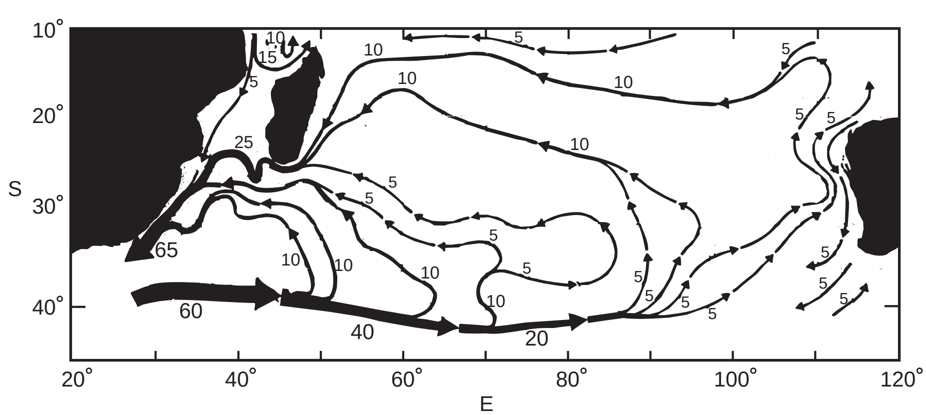

Figure 2 The baroclinic volume transport for the upper 1000 m of the South Indian Ocean. Values are in units of $10^6\,m^3\,s^{-1}$. Note the very small contribution coming from the Mozambique Channel and the concentration of the recirculation in the South West Indian Ocean west of 70°E. This transport pattern, averaged over a long period, is not to be confused with the depictions of instantaneous currents in **Figures 1** and **4**. (After Stramma and Lutjeharms (1997) *Journal of Geophysical Research* 102(C3): 5513–5530. © American Geophysical Union.)

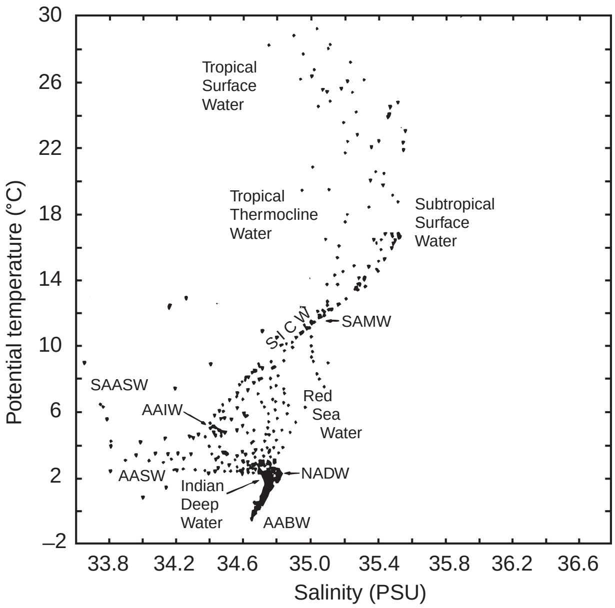

Figure 3 The relationship of potential temperature and salinity for waters in the western Indian Ocean. Some of the characteristic water masses to be found here are SICW, South Indian Central Water; SAMW, Subantarctic Mode Water; NADW, North Atlantic Deep Water; AABW, Antarctic Bottom Water; AASW, Antarctic Surface Water; AAIW, Antarctic Intermediate Water; and SAASW, Subantarctic Surface Water. (After Gordon *et al.* (1987) *Deep-Sea Research* **34**(4): 565–599. © Elsevier Science.)

seasonally varying monsoonal winds of the North Indian Ocean. The average air motion over the South Indian Ocean is dominated by a large-scale, anticyclonic circulation around a high-pressure system centered south-east of the island of Madagascar. This flow generally is stronger in austral summer than in winter. Strongest winds ($24\,\mathrm{m\,s^{-1}}$) are found at 50°S latitude in summer, and weakest at 35°S ($2\,\mathrm{m\,s^{-1}}$). A band of minimum wind stress extends across this ocean at 35°S. Next to the continental land masses the winds are usually aligned with the coasts. Apart from driving the surface currents, the atmosphere also has a considerable effect on the formation of certain water masses (**Figure 3**) that are typical for the region.

This temperature–salinity portrayal indicates the characteristic for each specific water mass in this ocean region. The fresher Tropical Surface Water is formed north of 20°S where there is an excess of precipitation over evaporation; Subtropical Surface Water is formed between 28° and 38°S, where this ratio is reversed. Subtropical Surface Water is found as a shallow subsurface salinity maximum in regions to the north and south of its region of formation. Intermediate waters lie at depths between 1000 and 2000 m and consist of Antarctic Intermediate Water and North Indian Intermediate Water (also called Red Sea Water). The former subducts between the Antarctic Polar Front and the Subtropical Convergence; the latter is formed owing to very high rates of evaporation in the Red Sea, the Arabian Sea and the Persian Gulf. Central Water, lying between the surface and the intermediate waters, is a mixture of these two. Below the intermediate waters are Indian Deep Water and North Atlantic Deep Water, each formed by subduction in the respective ocean regions after which they are named. All these respective water masses are involved in some way or other in the source currents of the Agulhas Current.

Sources of the Agulhas Current

According to the transport portrayed in **Figure 2**, 30% of the volume flux of the Agulhas Current derives from east of Madagascar, only 13% comes through the Mozambique Channel, and 67% is recirculated in a South West Indian Ocean subgyre. Note, however, that the inflow from east of Madagascar does not necessarily come from the East Madagascar Current (see **Figure 1**).

The southern limb of the East Madagascar Current starts at the bifurcation point of the South Equatorial Current at about 17°S along the east coast of Madagascar. Its surface speed here is roughly $1\,\mathrm{m\,s^{-1}}$, increasing downstream to about $1.5\,\mathrm{m\,s^{-1}}$. The current is very stable in both flux and trajectory and exhibits no clear seasonality in any of its characteristics. Using the $0.5\,\mathrm{m\,s^{-1}}$ isotach as the outer limits of the current, it is 75 km wide, 200 m deep, and its core lies 50 km offshore. It carries Tropical as well as Subtropical Surface Water with a total volume transport of $21 \times 10^6\,\mathrm{m^3\,s^{-1}}$ (i.e., 21 Sv). Where it overshoots the end of the shelf of Madagascar it retroflects, with most of its waters subsequently heading eastwards (**Figure 4**). There may be some leakage of East Madagascar Water into the Agulhas Current by way of rings and filaments, but this constitutes an insignificant contribution. The wider flow east of Madagascar, up to 240 km offshore, is $41 \times 10^6\,\mathrm{m^3\,s^{-1}}$. A substantial part of this more extensive flow may eventually make its way into the Agulhas Current (**Figures 2** and **4**).

The flow through the Mozambique Channel was once thought to be the major contributor to the flux of the Agulhas Current. Now it is considered to be minor (**Figure 2**). The entire existence of a consistent, continuous Mozambique Current, flowing along the African coastline, has in fact been called into question.

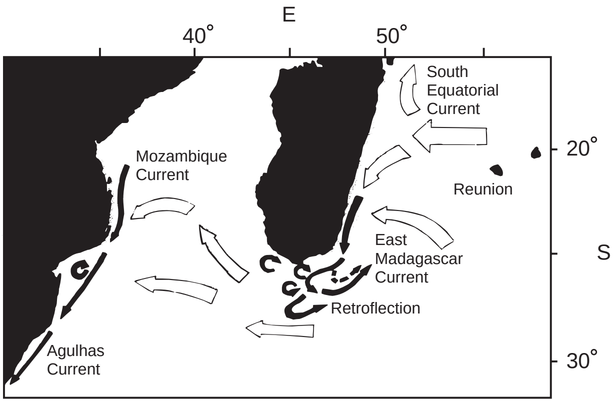

Figure 4 A conceptual portrayal of the flow regime in the source regions of the Agulhas Current. Narrow, intense currents are shown by black arrows. The East Madagascar Current is a miniature western boundary current that retroflects south of Madagascar. (After Lutjeharms *et al.* (1981) *Deep-Sea Research* **28**(9): 879–899. © Elsevier Science.)

The northern mouth of the Mozambique Channel is largely closed to subsurface flow by bottom ridges shallower than 2000 m, except at its western side. The surface circulation in the northern part of the channel is anticyclonic to an estimated depth of 1000 m. The eastern side of this flow, which might be the start of a Mozambique Current, is 250 km wide, has a surface speed of $0.3\,\mathrm{m\,s^{-1}}$ and a volume flux of $6\times10^6\,\mathrm{m^3\,s^{-1}}$. The water masses here are characteristic of the monsoonal regime to the north with no Antarctic Intermediate Water. There is some evidence for the presence of this water mass in the central part of the channel, but there still is no North Atlantic Deep Water. The rest is essentially Subtropical Surface Water of the South Indian variety. Occasional strong flows of $2\,\mathrm{m\,s^{-1}}$ have been observed off the African coastline in this central part of the channel, but this is extremely variable. The southern third of the channel has all the thermohaline characteristics of the South West Indian Ocean, including the presence of North Atlantic Deep Water. Net volume flux through the southern mouth of the channel seems to be very changeble. Calculations have varied from $26\times10^6\,\mathrm{m^3\,s^{-1}}$ southward to $5\times10^6\,\mathrm{m^3\,s^{-1}}$ northward, above 1000 m.

The best-substantiated characteristic of the circulation in the Mozambique Channel is therefore its very high mesoscale variability. This argues against a persistent western boundary current and instead suggests a series of eddies moving southward down the channel. This scenario is consistent with most available observations and also some numerical models.

Northern Agulhas Current

Water from the South West Indian Ocean subgyre feeds into the Agulhas Current along its full length, but at a latitude of 27°S this current is nonetheless thought to be fully constituted (**Figure 5**).

This northern part of the Agulhas Current is characterized in particular by an extremely stable trajectory; its core meanders less than 15 km to either side. This stability is thought to be due to the strong slope of the continental shelf along which it flows. The current has a well-developed, inshore thermal front that meanders somewhat more extensively. The surface characteristics of the current are given in **Table 1**.

Surface temperatures decrease by about 2°C downstream. In the north they are at a maximum of 28°C in February and a minimum of 23°C in July. At Port Elizabeth, where the southern Agulhas Current starts, the maximum temperature is 25°C in January, with a minimum of 21°C in August. Surface salinities decrease from 35.5 PSU in the north to 35.3 PSU in the south.

At Durban the core of the current usually lies 20 km offshore and penetrates to a depth of 2500 m (see **Figure 5**). Between the $0.5\,\mathrm{m\,s^{-1}}$ isotachs it is

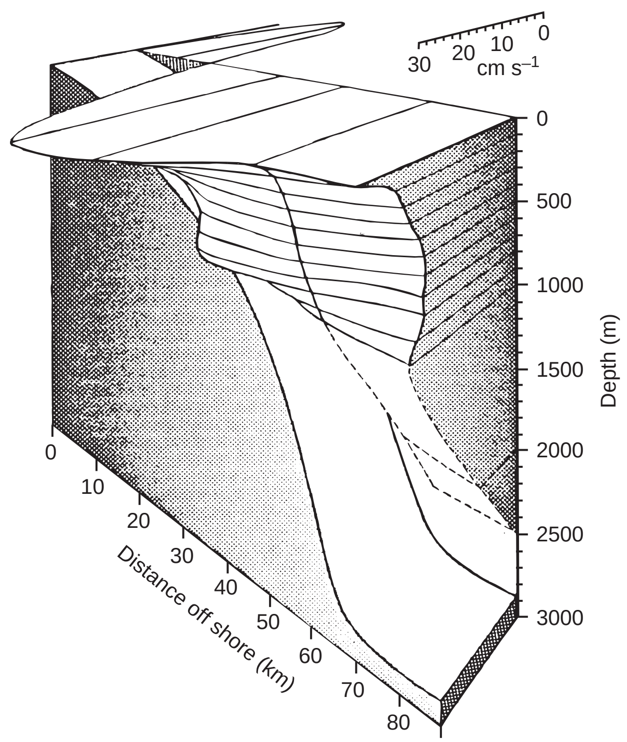

Figure 5 The spatial velocity structure of the northern Agulhas Current at Durban based on direct current measurements during a research cruise. Speeds below 1000 m have been estimated using a geostrophic calculation and are less certain. (After Duncan (1970) PhD dissertation, University of Hawaii.)

Table 1 Kinematic characteristics of the upper layers of the northern Agulhas Current

	Mean	*SD*	*Minimum*	*Maximum*
Peak speed in current core ($m\,s^{-1}$)	1.36	0.30		2.45
Current core offshore distance (km)	52	14	30	>100
Distance offshore $0.5\,m\,s^{-1}$ (km)	35	14	10	70
Distance offshore $1.0\,m\,s^{-1}$ (km)	42	14	25	95
Core width, between $1.0\,m\,s^{-1}$ isotachs (km)	34	15	10	>60
Distance offshore temperature max. (km)	58	20	35	>100
Distance offshore 15°C/200 m intersection (km)	50	15	25	90
Distance offshore 35.35 PSU salinity/200 m (km)	47	13	23	>100

After Pearce (1997), *Journal of Marine Research* 35(4): 731–753.

90 km wide; its offshore termination being more disperse than its strong inshore edge. Its core slopes so that at 900 m depth it lies 65 km offshore. Its total volume flux is $73\times10^6\,m^3\,s^{-1}$ and this increases by an estimated $6\times10^6\,m^3\,s^{-1}$ for every 100 km distance downstream in the northern Agulhas Current. Surface speeds at its core usually lie between 1.4 and $1.6\,m\,s^{-1}$, with occasional peaks of up to $2.6\,m\,s^{-1}$. Neither these velocities nor the volume fluxes show any discernible seasonality. The northern Agulhas Current is underlain by an opposing undercurrent at 1200 m that carries $6\times10^6\,m^3\,s^{-1}$ water equatorward at a rate of about $0.3\,m\,s^{-1}$. It consists partially of modified North Indian Intermediate Water.

The invariant path of the northern Agulhas Current is interrupted during about 20% of the time by an intermittent, solitary meander – the Natal Pulse – that originates at the Natal Bight, an offset in the coast north of 30°S (see **Figure 6**). It translates downstream at a very steady 20 km per day, continuously growing in its lateral dimensions. On its landward side it encloses a cyclonic eddy that creates a strong coastal countercurrent as the Natal Pulse passes. This meander is triggered at the Natal Bight whenever the current intensity there exceeds a

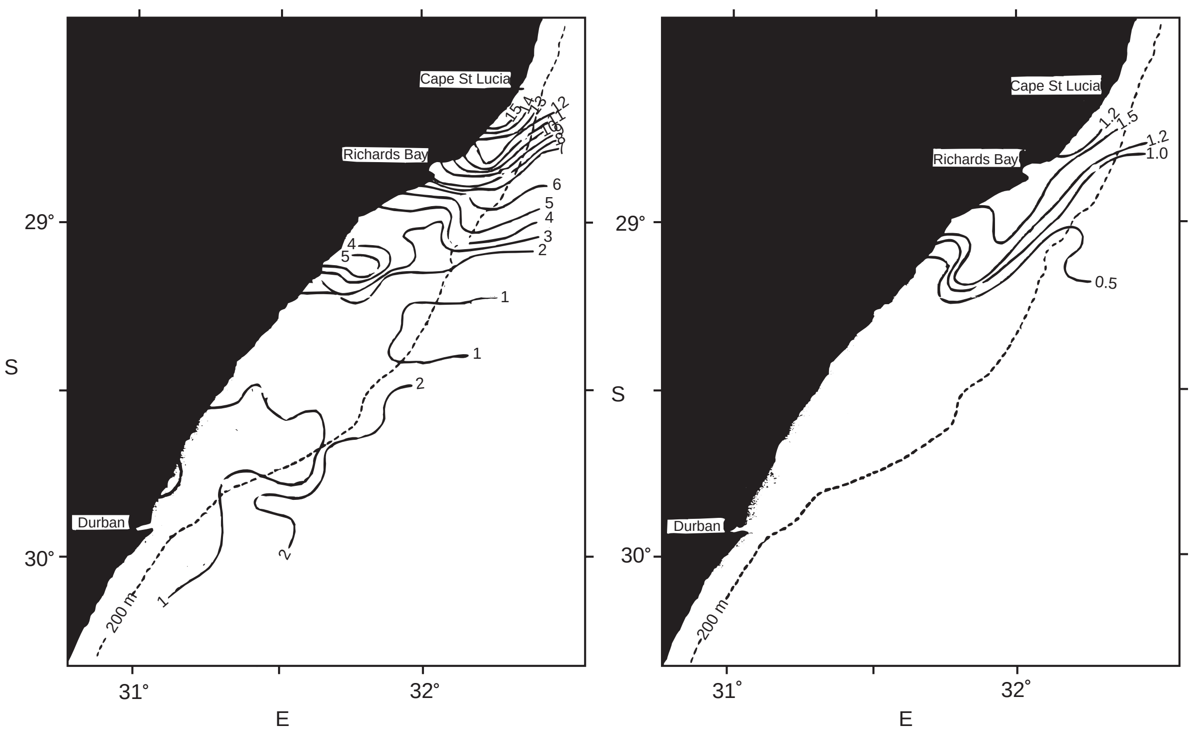

Figure 6 Current-induced upwelling in the Natal Bight off south-eastern Africa. The left panel gives the distribution of nitrate (in $\mu mol\,l^{-1}$) at 10 m depth and the right hand panel the simultaneous distribution of chlorophyll *a*. The active upwelling cell off Cape St Lucia with high nitrates and chlorophyll *a* is well circumscribed. (After Lutjeharms *et al.* (2000) *Continental Shelf Research* 20(14): 1907–1939. © Elsevier Science.)

certain threshold, allowing baroclinic instability to develop away from the constraining shelf slope. The Natal Pulse is an important component of the current system since it may cause upstream retroflection at the Agulhas Plateau (see **Figure 1**) and may precipitate ring shedding at the Agulhas retroflection, far downstream.

Flow over the shelf adjacent to the northern Agulhas Current is dependent on the shelf morphology. Where the shelf is narrow, the flow is mostly parallel to the current. Over the Natal Bight, where the shelf is wider, the flow consist of cyclonic eddies. At the northern end of the Natal Bight, the current forces inshore upwelling (**Figure 6**).

The water in this upwelling cell may be 5°C colder than the adjacent current, have a high nutrient content, and exhibit enhanced biological primary productivity. The cold water thus upwelled flows over the bottom of the whole Natal Bight, strengthening the vertical layering over this shelf region. Off Durban a recurrent lee eddy is often observed.

Seaward of the Agulhas Current, off the Mozambique Ridge (see **Figure 1**), a large number of very intense deep-sea eddies have been observed. They may be at least 2000 m deep, 100 km in diameter, have surface speeds of $1\,\mathrm{m\,s^{-1}}$ and circular transports of between 6×10^6 and $18\times10^6\,\mathrm{m^3\,s^{-1}}$. Their lifetimes are estimated to be 1–3 years. Most of those observed are cyclonic, although a few anticyclonic ones have been seen. They seem to come from both the Mozambique Channel and from east of Madagascar, but their true origins remain unknown.

Southern Agulhas Current

In contrast to the northern Agulhas Current, the southern Agulhas Current is characterized by wide meanders as it flows past the Agulhas Bank south of Africa (see **Figure 1**). Meanders are present along this shelf edge at least 65% of the time. They have an average wavelength of 300 km and a phase speed that varies from 5 to 23 km per day.

Meanders usually have a trailing plume and an embedded, cyclonic lee eddy (**Figure 7**). There is evidence that these eddies are preferentially clustered in the eastern bight of the Agulhas Bank (see **Figure 1**). The dimensions of all these shear edge features change markedly with distance downstream (see **Table 2**).

Sea surface temperatures also change more readily with distance downstream here than they do in the northern Agulhas Current. Sea surface temperatures in the southern Agulhas Current reach a maximum of 26°C at Algoa Bay in February; 23°C off the southern tip of the Agulhas Bank. In August these temperatures are 21°C and 17°C, respectively.

The volume flux of the Agulhas Current off the southern tip of the Agulhas Bank has been estimated at $70\times10^6\,\mathrm{m^3\,s^{-1}}$ down to 1500 m, i.e., about the same as that of the current to its full depth at Durban. Even though there is this increase, it seems that the increase per unit distance downstream found in the northern Agulhas Current is not maintained in its southern part. Water masses in the current are generally the same in the northern and the southern part. The presence of Tropical Surface

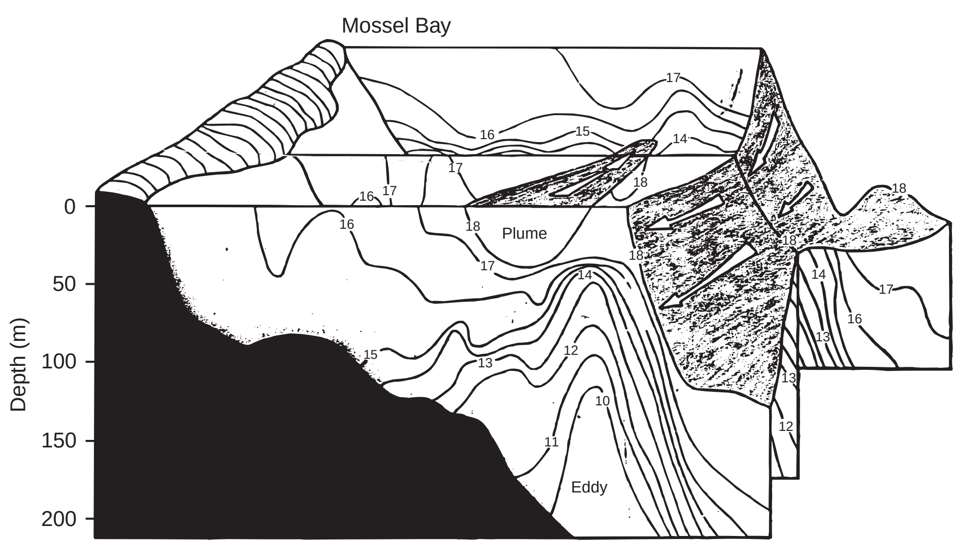

Figure 7 Three vertical temperature sections across the Agulhas Bank picture the thermal composition of the southern Agulhas Current, a shear-edge eddy, and its associated plume. The Agulhas Current lies outside the 18°C envelope. The plume has water warmer than 18°C while the core of the eddy has water colder than 10°C. (After Lutjeharms *et al.* (1989) *Continental Shelf Research* **9**(7): 1570–1583. © Elsevier Science.)

Table 2 Dimensions of shear edge features along the landward edge of the southern Agulhas Current

	Port Elizabeth	*Tip of Agulhas Bank*
Plume lengths at surface (km)	100	162
Plume widths at surface (km)	27	37
Diameter of enclosed eddy (km)	27	51
Plume dispersion from current (km)	50	150

After Lutjeharms *et al.* (1989) *Continental Shelf Research* 9(7): 597–616.

Water is maintained in the southern part, as are remnants of North Indian Intermediate Water (or Red Sea Water). Tropical Surface Water is mostly found at the inshore side of the current and derives from the Mozambique Current. Its presence and volume seem to be intermittent.

Some of the surface plumes generated by meanders in the far southern reaches of the Agulhas Current are advected past the western edge of the Agulhas Bank as Agulhas filaments (see **Figure 1**). They are present about 60% of the time and carry substantial amounts of heat that are rapidly lost to the much colder atmosphere. They also carry about $3\text{–}9 \times 10^{12}$ kg of salt per year into the South Atlantic; salt in excess to that of the waters already present there. On average they are 50 km wide and 50 m deep.

The southern Agulhas Current influences the water masses over the adjacent Agulhas Bank in three ways. First, plumes of warm Agulhas surface water may extend over the bank, heating the top layers (see **Figure 7**). Second, current-driven upwelling takes place off the far eastern side of the Agulhas Bank (see **Figure 1**) and this water flows westward and covers the greater part of the bottom of the shelf. This process cools the water column from below, leading to intense seasonal thermoclines over the Agulhas Bank. Third, most of the mean flow over the eastern part of this shelf is parallel to the current. At the southern tip of the Agulhas Bank, the current detaches from the shelf edge.

The Agulhas Retroflection

The region where the Agulhas Current then terminates south of Africa is characterized by its extremely high levels of mesoscale variability (**Figure 8**).

The measured eddy kinetic energy is higher here than in any comparable western boundary current such as the Kuroshio or the Gulf Stream. This is due to a number of dynamical traits of the current retroflection. First, the continuous progradation, or westward penetration, of the Agulhas retroflection loop into the South Atlantic Ocean causes substantial levels of variability. The loop has an average diameter of 340 km ($\pm$70 km) and progrades westward at about 10 km per day. The outer limits to its movement are 10° and 21°E. At its furthest extent a ring is shed by loop occlusion. This happens between 4 and 9 times per year. This ring spawning activity adds considerably to the general variability. Ring shedding events are usually preceded by the arrival of a Natal Pulse on the Agulhas Current. The average lag time between initiation of a Natal Pulse off the Natal Bight and the shedding of a ring at the retroflection is 165 days. Between a newly formed ring and the reconstituted retroflection loop, a wedge of Subtropical Surface Water usually penetrates northward. Its water has a temperature of 17°C and salinity lower than 34.9 over the top 100 m, also adding to the variability of the region.

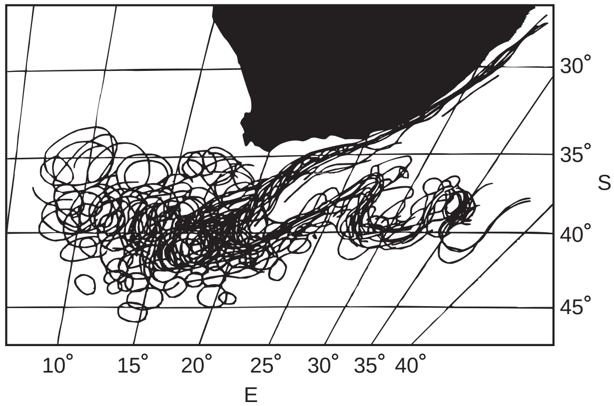

Figure 8 The high levels of mesoscale variability that are characteristic of the Agulhas Current retroflection and the Agulhas Return Current are here portrayed by the superimposed thermal borders at the sea surface as observed for a period of one year. The inshore border of the northern Agulhas Current is particularly stable, that of the southern Agulhas Current less so, whereas the Agulhas Return Current exhibits a tendency to prefer certain meanders. The Agulhas retroflection has a range of locations and is attended by a host of rings (to the north) and eddies (to the south). (After Lutjeharms and van Ballegooyen (1988) *Journal of Physical Oceanography* **18**(11): 1570–1580.)

Newly formed rings retain the hydrographic and kinematic characteristics of the southern Agulhas Current (**Table 3**). Since the heat loss from such a ring may be between 80 and 160 W m^{-2} and since there is substantial evaporation in the region, the temperature and salinity of the upper layers of the features are considerably modified near the retroflection region. Rings are about 320 km ($\pm$100 km) in diameter at the sea surface. Estimated by the location of their maximum azimuthal speeds, the

Table 3 Thermohaline characteristics of the principal water masses found at the Agulhas Current retroflection and vicinity

	Temperature range (°C)	*Salinity range (PSU)*
Surface Water	16.0 to 26.0	>35.50
Central Water		
South East Atlantic Ocean	6.0 to 16.0	34.50 to 35.50
South West Indian Ocean	8.0 to 15.0	34.60 to 35.50
Antarctic Intermediate Water		
South East Atlantic Ocean	2.0 to 6.0	33.80 to 34.80
South West Indian Ocean	2.0 to 10.0	33.80 to 34.80
Deep Water		
North Atlantic Deep Water (SE Atlantic)	1.5 to 4.0	34.80 to 35.00
Circumpolar Deep Water (SW Indian)	0.1 to 2.0	34.63 to 34.73
Antarctic Bottom Water	− 0.9 to 1.7	34.63 to 34.72

After Valentine *et al.* (1993) *Deep-Sea Research* 40(6): 1285–1305. © Elsevier Science.

diameters are a reduced 240 km ($\pm$ 40 km). These radial speeds lie between 0.3 and 0.9 m s^{-1}. The mean depth of the 10°C isotherm in Agulhas rings, a proxy for the geostrophic speed of their water masses, is 650 m ($\pm$ 130 m). Further properties, as estimated by a number of investigators, are given in **Table 4**.

Rings move off into the South Atlantic Ocean at speeds of 4–8 km per day. Maximum translation rates of up to 16 km per day have been observed. They lose 50% of their sea surface height – and therefore by inference of their energy – during the first 4 months of their lifetime. A full 40% of rings never seem to leave the Cape Basin, off the south-eastern coast of Africa, at all but totally disintegrate here. This decay may well be enhanced by the splitting of rings. This process seems to be largely induced by rings passing over prominent features of the bottom topography such as seamounts. This rapid dissipation of these features means that a considerable part of all the excess salt, heat, energy, and vorticity carried by the rings is deposited exclusively in this corner of the South Atlantic. The remaining rings seem to have lifetimes between 2 and 3 years. They move westward across the full width of the South Atlantic Ocean, slightly to the left of the general background flow. A few of them interact with the upwelling front off the south-eastern coast of Africa, with upwelling filaments occasionally being wrapped around passing rings. These Agulhas rings play a crucial role in the interbasin exchange of waters between the South Indian and South Atlantic Oceans. This is partially quantified in **Table 5**.

Agulhas Return Current

That part of the Agulhas Current not involved in ring production flows back in an easterly direction on having successfully negotiated the retroflection. Here also there are very high levels of mesoscale variability with substantial meandering and eddies being shed to both sides of the Agulhas Return Current/Subtropical Convergence. Much of this meandering is brought about by the variable bathymetry over which the current has to pass.

The first obstacle to a purely zonal flow for the Agulhas Return Current is the Agulhas Plateau (see **Figure 1**). Here it carries out a northward meander of 290 $\pm$ 65 km. Cold eddies are frequently formed here with diameters of 280 $\pm$ 50 km, but rapidly warm to become indistinguishable from ambient surface waters. Warm eddies may in turn be shed to the south. One such eddy that has been observed closely remained in roughly the same position for 2 months, rotated every 3 days, and had a volume flux of $32\times10^6\,m^3\,s^{-1}$ to a depth of 1500 m.

Table 4 Physical properties of Agulhas rings as furnished by a number of independent investigators, calculated with respect to the characteristics of water in the South East Atlantic Ocean

Investigators	*Heat flux (10^{-3} PW)*	*Salt flux (10^5 kg/s)*	*Available potential energy (10^{15} J)*	*Kinetic energy (10^{15} J)*
Olson and Evans (1986)			30.5–51.4	6.2–8.7
Duncombe Rae *et al.* (1989)	25	6.3		
Duncombe Rae *et al.* (1992)			38.8	2.3
Van Ballegooyen *et al.* (1994)	7.5	4.2		
Byrne *et al.* (1995)			18	4.5
Clement and Gordon (1995)			7.0	7.0
Duncombe Rae *et al.* (1996)	1.7	1.1	11.3	2.0
Goni *et al.* (1997)			24	
Garzoli *et al.* (1996)	1.0–1.6	0.7–1.0	2.8–3.8	

After De Ruijter WPM *et al.* (1999) Indian–Altantic inter-ocean exchange: dynamics, estimation and impact. *Journal of Geophysical Research* 104(C9): 20885–29911. © American Geophysical Union, where full references can be found.

Table 5 Estimates of interbasin volume transport between the South Indian and the South Atlantic Oceans caused by ring shedding. The values were calculated by the investigators named here. For full references see De Ruijter *et al.* (1999)

Investigators	*Volume transport per ring ($10^6\,m^3\,s^{-1}$)*	*Referenced to*
Olson and Evans (1986)	0.5–0.6	$T > 10°C$
Duncombe Rae *et al.* (1989)	1.2	Total
Gordon and Haxby (1990)	1.0–1.5	$T > 10°C$
	2.0–3.0	Total
McCartney and Woodgate-Jones (1991)	0.4–1.1	Total
Van Ballegooyen *et al.* (1994)	1.1	$T > 10°C$
Byrne *et al.* (1995)	0.8–1.7	1000 db
Clement and Gordon (1995)	0.45–0.90	1500 db
Duncombe Rae *et al.* (1996)	0.65	Total
Goni *et al.* (1997)	1.0	$T > 10°C$

After De Ruijter WPM *et al.* (1999) Indian–Atlantic inter-ocean exchange: dynamics, estimation and impact. *Journal of Geophysical Research* 104(C9): 20885–20911. © American Geophysical Union.

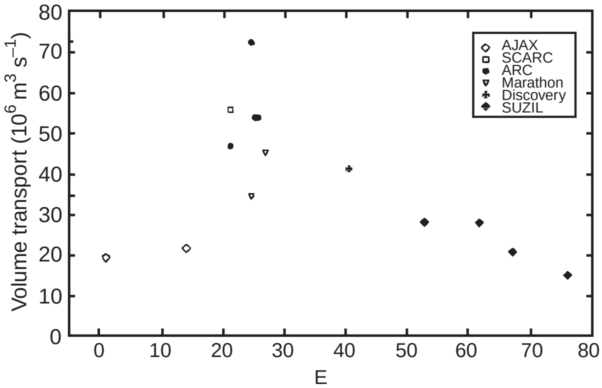

Figure 9 The nature of the volume flux along the Subtropical Convergence south of Africa, as established by a number of individual research cruises (shown in the box). Transport is in units of $10^6\,m^3\,s^{-1}$ and has been calculated to a depth of 1500 m. The influence of the Agulhas Current is felt from 20°E eastwards, but by the 70°E meridian it has been dissipated completely. This may therefore be considered the termination of the Agulhas Return Current and the start of the South Indian Ocean Current. (After Lutjeharms and Ansorge *Journal of Marine Systems*, in press.)

Downstream of the Agulhas Plateau the next meander lies at a distance of 450 ± 110 km. These meanders move upstream at about half a wavelength per season. Upstream of the Plateau there are also westward-propagating Rossby waves on the Agulhas Return Current/Subtropical Convergence. However, the direct correlation between the Agulhas Return Current and the Subtropical Convergence is not always straightforward. Sometimes they are in close juxtaposition, sometimes not. When they are not, two separate fronts, or even multiple fronts, may be formed (**Table 6**).

The Agulhas Current has a considerable effect on the Subtropical Convergence, forcing it to lie 5° of latitude farther south than in the South Atlantic Ocean and increasing its surface gradients so that a meridional gradient of 5°C in 35 km is not unknown.

The Agulhas Return Current starts off with characteristics nearly identical to those of the Agulhas Current. South of Africa it may exhibit a surface speed of $1.3\,m\,s^{-1}$ and a volume transport of $40 \times 10^6\,m^3\,s^{-1}$ to 1000 m. The parallel flow along the Subtropical Convergence would be $16–20 \times 10^6\,m^3\,s^{-1}$ at the same time. All these flow characteristics decrease rapidly as the current progresses eastward (**Figure 9**). By about 55°E, the surface velocity has reduced to $0.4\,m\,s^{-1}$ and the volume flux to about $19 \times 10^6\,m^3\,s^{-1}$. By a longitude of 70°E, at the Kerguelen Plateau, little of the Agulhas characteristics remain along the Subtropical Convergence, all of the Agulhas water having leaked off into the South West Indian Ocean subgyre. The speed, volume transport, as well as mesoscale variability associated with the Agulhas Return Current will all have declined here to values observed in the

Table 6 The geographic location and the thermal characteristics of the surface expressions of the Agulhas Front as well as the Subtropical Convergence south of Africa. Values for the Agulhas Front were based on 24 crossings, that of the Subtropical Convergence on 70. Values in parentheses denote standard deviations for the calculated averages

	Latitudinal position				*Temperature*				
	From	*To*	*Middle*	*Width (km)*	*From*	*To*	*Middle*	*Range*	*Gradient (°C km^{-1})*
Agulhas Front	39°09′	40°01′	39°37′	96.3	21.0	15.7	18.4	5.4	0.102
	(01°16′)	(01°06′)	(01°14′)	69.1	(1.6)	(1.5)	(1.2)	(1.6)	0.106
Subtropical Convergence	40°35′	42°36′	41°40′	225.1	17.9	10.6	14.2	7.3	0.047
	(01°23′)	(01°32′)	(01°19′)	140.6	(2.1)	(1.8)	(1.7)	(1.9)	(0.043)

After Lutjeharms and Valentine (1984) *Deep-Sea Research*, 31(12): 1461–1476. © Elsevier Science.

south-eastern Atlantic Ocean, upstream of any influence from the Agulhas Current. The Agulhas Return Current can therefore be considered to have terminated here. The continuing flow along the Subtropical Convergence east of here is known as the South Indian Ocean Current.

Conclusion

The Agulhas Current is unusual as a western boundary current for a number of reasons. First, because the African continent terminates at relatively low latitudes, the current penetrates freely into the adjacent ocean basin and a substantial leakage between basins is feasible. Second, through the process of ring and filament shedding, an interaction between a western boundary current and an extensive coastal upwelling regime is brought about that is geographically not possible elsewhere. Third, the very stable nature of the northern Agulhas Current and its characteristic Natal Pulse creates a dynamic environment in which mesoscale disturbances can have profound circulatory effects downstream. The contemporary ignorance about the East Madagascar Current, about the circulation of the Mozambique Channel, and about the origin of midocean eddies in the South West Indian Ocean needs to be eliminated. Only then will a more realistic concept of the interactions between elements of the greater Agulhas Current system become possible.

See also

Mesoscale Eddies. Ocean Circulation. Water Types and Water Masses.

Further Reading

De Ruijter WPM, Biastoch A, Drijfhout SS *et al*. (1999) Indian–Atlantic inter-ocean exchange: dynamics, estimation and impact. *Journal of Geophysical Research* 104: 20885–20911.

Lutjeharms JRE (1996) The exchange of water between the South Indian and the South Atlantic. In: Wefer G, Berger WH, Siedler G and Webb D (eds) *The South Atlantic: Present and Past Circulation*, pp. 125–162. Berlin: Springer-Verlag.

Lutjeharms JRE (2001) *The Agulhas Current*. Berlin: Springer-Verlag.

Shannon LV (1985) The Benguela Ecosystem. 1. Evolution of the Benguela, physical features and processes. *Oceanography and Marine Biology, An Annual Review* 23: 105–182.

Shannon LV and Nelson G (1996) The Benguela: large scale features and processes and system variability. In: Wefer G, Berger WH, Siedler G and Webb D (eds) *The South Atlantic: Present and Past Circulation*, pp. 163–210. Berlin: Springer-Verlag.

AIRCRAFT REMOTE SENSING

L. W. Harding, Jr and W. D. Miller, University of Maryland, College Park, MD, USA
R. N. Swift and C. W. Wright, NASA Goddard Space Flight Center, Wallops Island, VA, USA

Copyright © 2001 Academic Press

doi:10.1006/rwos.2001.0425

Introduction

The use of aircraft for remote sensing has steadily grown since the beginnings of aviation in the early twentieth century and today there are many applications in the Earth sciences. A diverse set of remote sensing uses in oceanography developed in parallel with advances in aviation, following increased aircraft capabilities and the development of instrumentation for studying ocean properties. Aircraft improvements include a greatly expanded range of operational altitudes, development of the Global Positioning System (GPS) enabling precision navigation, increased availability of power for instruments, and longer range and duration of missions. Instrumentation developments include new sensor technologies made possible by microelectronics, small, high-speed computers, improved optics, and increased accuracy of digital conversion of electronic signals. Advances in these areas have contributed significantly to the maturation of aircraft remote sensing as an oceanographic tool.

Many different types of aircraft are currently used for remote sensing of the oceans, ranging from balloons to helicopters, and from light, single engine piston-powered airplanes to jets. The data and information collected on these platforms are commonly used to enhance sampling by traditional oceanographic methods, giving increased spatial and temporal resolution for a number of important properties. Contemporary applications of aircraft remote sensing to oceanography can be grouped